ELSEVIER

Journal of Chromatography A, 910 (2001) 19–30

JOURNAL OF CHROMATOGRAPHY A

www.elsevier.com/locate/chroma

Quantitative FTIR detection in size-exclusion chromatography

Keivan Torabi[a], Askar Karami[a], Stephen T. Balke[a], Timothy C. Schunk[b,*]

[a]*Department of Chemical Engineering and Applied Chemistry, University of Toronto, Toronto, Ontario, Canada*
[b]*Imaging Materials and Media, Eastman Kodak Company, Rochester, NY, USA*

Received 26 June 2000; received in revised form 31 October 2000; accepted 6 November 2000

Abstract

With the increasing popularity of evaporative interfaces, detection using Fourier Transform Infrared (FTIR) spectrometry in the mid-infrared region is becoming more important in size-exclusion chromatography (SEC). FTIR spectrometry is a powerful, and potentially very widely applicable, method for obtaining chemical functional group information for each molecular size fraction. Quantitative evaluation of polymer composition across the SEC chromatogram can provide more accurate characterization of heterogeneous polymer samples for problem solving and for material specification. The evaporative interface removes the SEC mobile phase at the exit of the column and deposits the eluting polymer as a continuous film stripe or as a series of discrete films on infrared transparent substrates. Initially this detection approach was used only for qualitative analysis. More recently, it is being used quantitatively. Previously we demonstrated that the quality of the film generated by the evaporative interface was critical to determining the suitability of the resulting FTIR spectra for quantitative analysis. In a continuation of this work, the objective of this paper is to develop a procedure for obtaining valid quantitative results for polymer blends with the interface. Experimental topics include improving the quality of polymer films by post-SEC treatments, off-line FTIR calibrating using other means to obtain high quality polymer films, and utilizing in-line SEC detectors in calibration. Interpretation aspects focus upon peak fitting of FTIR spectra, linear regression, partial least squares, and data pre-processing. PLS prediction with internal calibration using the second derivative of solvent-annealed film spectra was found to provide the best compromise between processing time, accuracy and precision.

Keywords: Fourier transform infrared spectroscopy; Detection, LC; Polymers

1. Introduction

In size-exclusion chromatography (SEC) analysis, variation in chemical composition or molecular architecture as a function of molecular size can cause conventional interpretation methods to fail. In addition, the ability to quantitatively determine the variation in chemical composition across an SEC chromatogram is often critical to developing accurate structure–property relationships. These two factors create two critical needs: a method of detection that can discern differences in composition for a variety of polymers and a quantitative approach which can interpret the resulting data.

Fourier Transform Infrared (FTIR) spectrometry is a detection method which potentially fits the first mentioned need. It is a powerful, and very widely applicable, method for obtaining chemical functional group information for polymeric materials. The

*Corresponding author. Tel.: +1-716-722-9508.
E-mail address: timothy.schunk@kodak.com (T.C. Schunk).

0021-9673/01/$ – see front matter
PII: S0021-9673(00)01122-5

direct interfacing of SEC and FTIR has evolved from two directions: in-line flow cells and solvent evaporation interfaces that can remove the solvent prior to FTIR spectral analysis. Low-volume flow cells offer continuous monitoring of the eluates with little loss of chromatographic resolution. However, application has been limited, due to the strong infrared absorption inherent in SEC eluents throughout much of the mid-infrared spectral range [1,2]. The evaporative interface currently offers the only practical method for using FTIR in SEC [3–6]. Such an interface allows full use of the mid-IR spectral range by providing analyte films free from solvent interference. The evaporative interface removes the SEC mobile phase at the exit of the column and deposits the eluting polymer as a continuous film stripe or as a series of discrete films on an infrared transparent substrate (e.g., germanium). Initially this detection approach was used only for qualitative analysis. More recently, it is being used quantitatively. Thus, satisfying the second need mentioned above, assessment and development of quantitative methods suited to interpretation of the resulting FTIR data, has become extremely important and is the main topic of this paper.

2. Theory

For the same polymer, the quantitative results obtained from use of the evaporative interface in SEC depend upon two major factors: the quality of the polymer films and the mathematical approach used in interpreting the data. These are discussed in turn below.

2.1. Spectral quality

When an evaporative interface is used, the evaporation conditions inside the interface combined with the properties of the polymer solution and the collection substrate determine the quality of the film obtained. Previously we have shown that the uniformity of the film and the presence of any bare spots greatly influence the resulting spectrum [7–10]. Refractive index variations due to film structures on the scale of the mid-IR wavelength range produce Christiansen scattering distortions [11,12]. These effects can produce significantly sloping spectral backgrounds and derivative-shaped absorbance bands.

A solvent annealing process can be used to improve film uniformity. It can even reduce the percentage of bare spots in the polymer films [8]. We have previously reviewed the impact of holes or bare spots in the polymer film deposits on the accuracy of the absorbance band intensity and showed that this effect is not significant for absorbance values less than 0.15 for films with as high as 40% bare area [10]. All spectra in this study were intentionally kept in the range of less than 0.15 maximum absorbance.

2.2. Quantitative interpretation

Quantitative interpretation of FTIR data proceeded in two steps: calibration and prediction. Fig. 1 shows the two major calibration methods used in this work: external calibration and internal calibration. For external calibration, polymer films of different thickness were cast from solution. The FTIR absorbance spectrum and the mass of each of a series of different films provided the needed data. Linear regression was used in two ways to establish the correlation: firstly, each spectrum was fit by the sum of Gaussian peaks and the area of a specific peak was regressed against polymer mass (regression LR:E1); secondly, the second derivative of absorbance with respect to wavelength was obtained for each spectrum using numerical differentiation and the area under the doubly differentiated peak was regressed against polymer mass (regression LR:E2) [13,14].

In the second type of calibration, internal calibration, the spectra were measured on successive fractions obtained from the evaporative interface and the mass of each fraction was obtained from area slices in the differential refractive index (DRI) chromatogram. Again two methods of quantifying the correlation were used: first, in a manner similar to that of LR:E2 the area under the doubly differentiated spectrum was regressed against polymer mass (regression LR:I); the second method involved using the spectrum obtained after the double differentiation and the polymer masses in a chemometric method known as partial least squares (PLS:I). Both regression and partial least squares have been well described in the published literature [13,14].

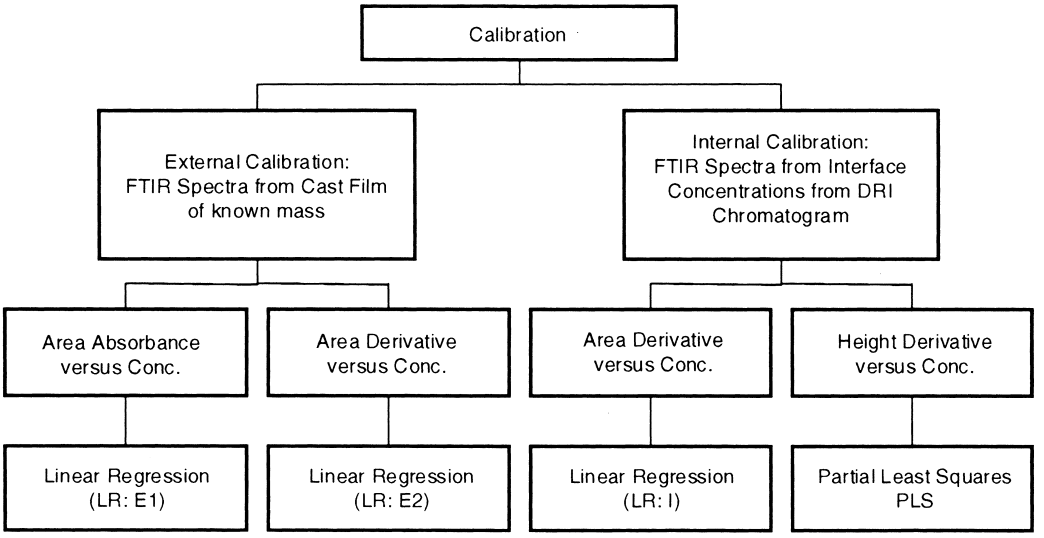

Fig. 1. Calibration approaches.

2.3. Assessment of quantitative methods

Assessment of accuracy (closeness to the true value) and precision (repeatability) were the focus. Accuracy was measured by considering that the values obtained from the DRI chromatogram were the ''true'' values.

Then, the accuracy of two measures were examined. The first was the deviation of the weight fraction of each polymer fraction j obtained by analysis of the FTIR spectrum calculated as a relative percent deviation (R_j):

$$R_j = 100\,\frac{w_{j,\mathrm{FTIR}} - w_{j,\mathrm{DRI}}}{w_{j,\mathrm{DRI}}} \quad (1)$$

where w_j is the weight fraction of component j (e.g. weight fraction of poly(methyl methacrylate)) where the method used to measure w_j is indicated by the subscript FTIR or DRI.

The second measure of accuracy examined was the bias in total mass collected by the interface. The relative percent deviation in total mass, R_m, was obtained from:

$$R_m = 100\frac{m_{\mathrm{FTIR}} - m_{\mathrm{DRI}}}{m_{\mathrm{DRI}}} \quad (2)$$

where m_{FTIR} is the mass obtained from summing the mass values obtained from each FTIR spectrum and m_{DRI} is the mass obtained from the area under the DRI chromatogram.

Precision was computed for total mass as the coefficient of variation (CV_m). Precision of individual fraction values varied with retention volume. With only three replicates available for each set of solvent evaporative conditions all three of these runs were plotted against retention volume to show the precision.

3. Experimental

3.1. Materials

Polystyrene (PS) NBS 706 was obtained from NIST (Washington, DC, USA) and poly(methylmethacrylate) (PMMA) broad standard lot 037B was obtained from Scientific Polymer Products (SP2) (Ontario, NY, USA).

3.2. Size-exclusion chromatography

SEC separations were performed on a three-column set of PLgel 10 μm 300×7.5 mm mixed bed columns (Polymer Laboratories, Amherst, MA, USA). A Waters 590 pump (Waters Associates, Milford, MA, USA) was used to deliver 1.0 ml/min

of freshly distilled helium sparged tetrahydrofuran (THF). HPLC grade THF (J. T. Baker, Phillipsburg, NJ, USA) was distilled from calcium hydride (Eastman Kodak Company, Rochester, NY, USA) to eliminate peroxides and water. Polymer samples at 5.00 mg/ml total concentration in THF were injected from a 100 μl loop using a Rheodyne (Cotati, CA, USA) injection valve. All samples were analyzed at least in triplicate. A second Rheodyne valve was used to switch the solvent flow after the columns to either a Waters Assoc. Model R401 DRI detector or the solvent–evaporation interface as shown in Fig. 2. The solvent flow path shown in Fig. 2 was configured to provide equal volume from the switching valve to either the DRI or solvent–evaporation interface.

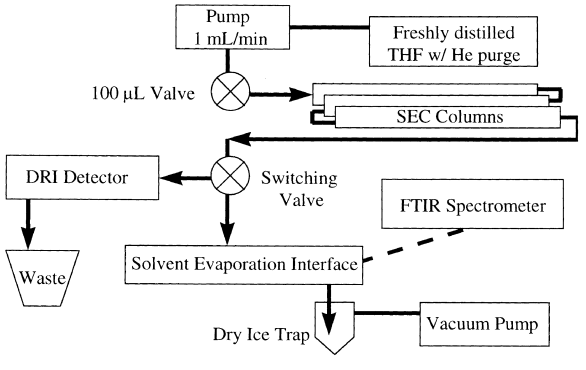

Fig. 2. Experimental system configuration with alternate DRI or solvent–evaporation-interface connection.

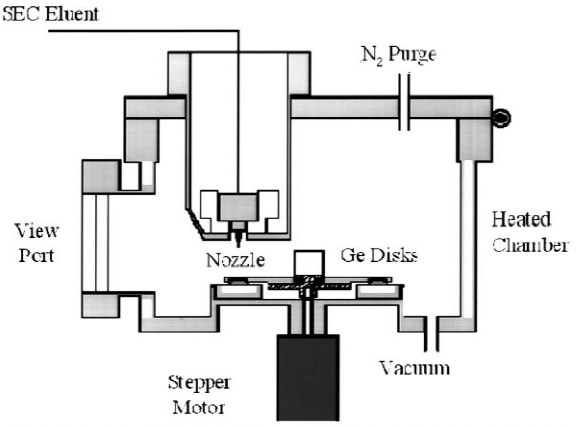

Fig. 3. Diagram of the solvent–evaporation interface.

3.3. Solvent evaporation interface

The results described in this work were generated using a custom built solvent–evaporation interface similar in basic design to that described by Dekmezian et al. [15]. A diagram of the solvent–evaporation interface is shown in Fig. 3. The interface consisted of a stainless steel temperature-controlled vacuum chamber. The temperature of the evaporation chamber was controlled by circulating silicone oil at 60°C with a Haake Model DC5-GH (Paramus, NJ, USA) circulating bath through the double walled chamber. During sample collection the chamber pressure was maintained at 25 Torr using a dry ice trapped vacuum pump to remove solvent vapor and a 4.5 l/min N_2 purge. The stainless steel sample collection wheel was 150 mm in diameter with 20 equally spaced wells holding 13×2 mm polished germanium (Ge) disks (Spectral Systems, Hopewell Junction, NY, USA) as collection substrates. The collection wheel was maintained at 90°C on a nickel-plated copper stage temperature controlled with silicone oil from a Haake Model A81 circulating bath. The SEC solvent stream was sprayed onto the Ge disks using a Sonotek Corp. (Poughkeepsie, NY, USA) 120 kHz ultrasonic nozzle at 0.50 W power. The nozzle temperature was stabilized at 30°C with a 40 psig N_2 stream inside the nozzle housing.

For each SEC analysis the interface chamber was equilibrated with the THF vapor of the SEC eluent for 17 min after sample injection prior to the start of sample collection (see Fig. 4). SEC samples were collected as 19 fractions each 20 s in duration across the SEC chromatogram by positioning the sample wheel with a computer controlled Slo–Syn stepper motor (Superior Electric, Bristol, CT, USA).

3.4. Sample preparation and FTIR analysis

After sample collection, a cover plate was placed over the sample wheel and the assembly removed from the collection chamber. To improve collected film uniformity and minimize IR scattering distortions, each Ge disk was briefly exposed to the vapor above refluxing dichloromethane (J.T. Baker) after the sample wheel was removed from the interface.

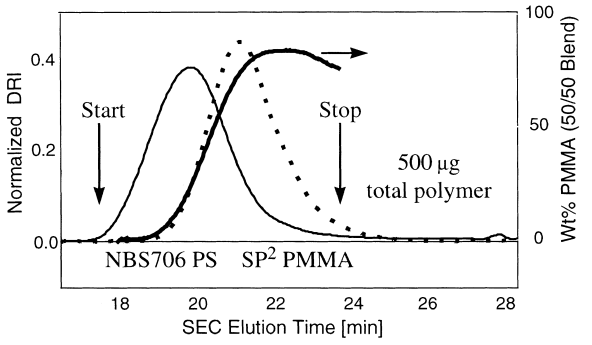

Fig. 4. Normalized DRI chromatograms of pure PS NBS 706 (———) and PMMA (· · ·) used in blend SEC experiments. The heavy line indicated on the right axis is the calculated weight percent PMMA present in a 50:50 blend sample across the SEC chromatogram. The solvent–evaporation interface was used to collect fractions from each SEC chromatogram between the indicated start and stop times for FTIR analysis.

After this solvent annealing, the sample wheel was placed on a similar stepper motor drive in the FTIR spectrometer. FTIR spectra were obtained at 8 cm^{-1} resolution with 32 co-averaged scans using Mattson WinFirst software. Spectra from manually cast calibration films were obtained with either a Mattson Galaxy 6020 or a Mattson Polaris Spectrometer (Madison, WI, USA). Spectra from SEC fraction films collected with the solvent–evaporation interface were obtained on a Mattson Polaris Spectrometer.

3.5. Data analysis

Spectral peak fitting was performed using PeakFit software (SPSS Inc., Chicago, IL, USA). Second derivatives of the IR absorbance spectra were determined numerically using a Savitsky–Golay algorithm with a second-degree five point smooth. Band area of each second derivative IR spectrum was determined as the baseline corrected area between the inflection points of the second derivative plot after multiplication by negative one. Partial Least Squares calibration models with mean centered second derivative spectra and quantitative calculations were performed using PLS IQ GRAMS/32 software (Galactic Industries Corp., Salem, New Hampshire, USA).

4. Results and discussion

4.1. Use of the liquid cell instead of the evaporative interface

IR solution spectra were obtained for a series of PMMA and PS samples in an off-line liquid cell. Dichloromethane was found to provide improved mid-IR transparency for absorbance bands of PS and PMMA. However, the background absorbance of the solvent significantly reduced the usable mid-IR window and produced many low level interfering bands. Although it was possible to obtain a linear calibration response for PMMA in the SEC solution concentration range, no usable calibration could be obtained for PS.

4.2. DRI analysis of the polystyrene/poly(methyl methacrylate) blends

SEC of polystyrene (PS) and poly(methylmethacrylate) (PMMA) blends were used to provide well controlled polymer composition variation across the chromatogram. Fig. 4 shows the comparison of individually obtained mass normalized DRI chromatograms of the reference PS and PMMA samples used in this study. For all samples a constant mass of polymer was injected into the SEC columns. Polymer blend composition was varied for different blend samples by changing the ratio of PS to PMMA in the blend solution. The heavy line in Fig. 4 shows the weight percent PMMA calculated using the DRI signals across the SEC chromatogram of a 50/50 blend of the PS and PMMA.

5. Film quality

5.1. Solvent–evaporation interface produced films

The properties of the polymer solution and the collection substrate combine with the interface conditions to provide films that are consistent in diameter, but variable in thickness and uniformity. As discussed, this adversely affects the quality of the IR spectra obtained, most obviously in terms of scattering distortions. Fig. 5 shows the typical improvement in spectral baseline, bandshape, and absorbance

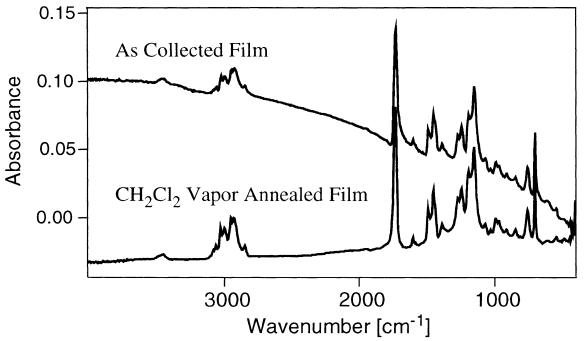

Fig. 5. Impact of solvent annealing on the IR scattering background for a 50:50 PS/PMMA blend fraction collected from SEC with the solvent–evaporation interface.

intensity obtained via the solvent annealing process used to improve film uniformity [8].

5.2. External calibration standards

Polymer film uniformity was also determined to be critical to the generation of external standards of manually cast polymer films for FTIR calibration. Table 1 shows the impact of changing casting conditions for the application of a measured volume polymer solution onto a heated germanium disk. It was determined that rapid evaporation provided more uniform films with less of a tendency to form a ''doughnut'' shaped deposit. In addition, centering of the cast film on the Ge disk was critical to providing consistent absorbance response.

The uniformity of the manually cast polymer film standards was evaluated by a masking experiment, as shown in Table 2. Four spectra were obtained for each cast film using a small diameter mask to provide IR transmission. As the mask opening was located at various positions around the perimeter of the film and absorbances obtained through the opening were compared to that obtained in the deposit

Table 1
Impact of polymer film manual casting conditions on PMMA absorbance band area at 1730 cm^{-1} from three replicates

Deposition procedure	Mean (AU cm^{-1})	C.V. (%)
Heat and centered	0.31	2.6
Heat, but off-center	0.13	5.4
IR heating	0.039	7.7

Table 2
Manually cast film uniformity determined from six replicates by a masking experiment for PMMA absorbance band area at 1730 cm^{-1}

FTIR spectrum location	Mean (AU cm^{-1})	C.V. (%)
Full field	0.31	3.0
Center	0.32	6.0
Edge at 0°	0.32	4.2
Edge at 120°	0.30	10.2
Edge at 240°	0.29	8.6

center, variations in the polymer film thickness were detectable. For accurate absorbance calculations, blank spectra were obtained from a clean Ge disk with the same masked area. With the data shown in Tables 1 and 2, it was possible to verify the quality and consistency of manually cast polymer films as standards for external calibration.

5.3. Spectral peak fitting

In order to provide accurate IR information, two spectral features must be mathematically determined for all spectra: the correct baseline and the absorbance band intensity. For the external standard, linear regression calibration approach (LR:E1) all spectra were fitted using fixed parameters in PeakFit Software. Baseline correction of a small IR region with Gaussian band-shape fitting of the 699 cm^{-1} band with PeakFit Software is shown in Fig. 6. Note that the best-fit baseline passes through some positive response regions. In addition, examination of a

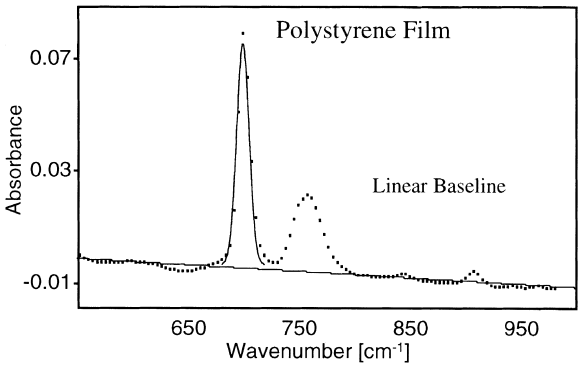

Fig. 6. Example result of PeakFit software baseline and Gaussian band fitting for a narrow region of a PS film spectrum.

broader frequency range for the spectrum may indicate that responses in the so-called fingerprint region 1000–1500 cm^{-1} may not have any points of zero absorbance response for baseline fitting and therefore the baseline shown in Fig. 6 may provide underestimates of band intensity. Use of the full spectrum further degrades the baseline fitting accuracy by emphasizing large-scale baseline shifts at the expense of accurate baselines in the vicinity of absorbance bands. Peak fitting of narrow spectral regions as shown in Fig. 6 was chosen as a compromise.

For LR:E2, LR:I, and PLS:I (external and internal calibration using 2nd derivative spectra), the spectra used to build the training set were modified using the second derivative of the absorbance spectra with a Savitsky–Golay second degree five point smooth. The second derivative approach reduces the impact of large-scale baseline variations on the relatively narrow absorbance bands.

5.4. Linear regression calibration

The resulting external calibration data and LR:E1 fits for a series of manually cast polymer films of PS and PMMA are shown in Fig. 7. For each polymer a strong absorbance band not overlapped by response from the other polymer blend component was selected for calibration.

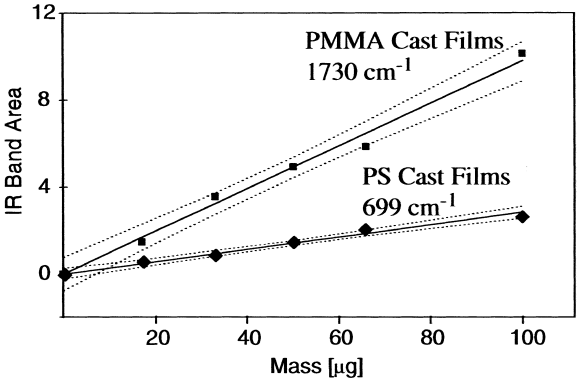

Fig. 7. Calibration plots of absorbance band areas determined with PeakFit software for manually cast polymer films. The dotted lines indicate 95% confidence interval ranges about the regression lines.

5.5. Quantitative analysis of composition across the chromatogram using LR and external calibration (LR:E1 and LR:E2)

The linear regression calibration equations using the area of Gaussian fit peaks from Fig. 7 were applied to quantify the polymer blend composition across the SEC chromatograms for a series of PS/PMMA blend ratios. For each sample the solvent-annealed polymer film spectra of each SEC fraction was analyzed for PS and PMMA mass content. The weight percent PMMA in each fraction was then calculated from these individual values. Figs. 8–10 show the results of three replicate analyses compared with the wt% PMMA calculated from the previously determined DRI chromatograms.

Agreement is excellent between the blend composition across the SEC chromatograms calculated from the independent DRI signals and the FTIR quantitation. The shapes of the composition curves agree for all blend samples even at long retention times where the total mass of polymer is less than 10 μg.

With the use of external calibration standards, the percent recovery of the solvent–evaporation interface can also be determined from summation of the individual fraction masses. For the 50:50 blend samples (Fig. 8) an average value of 101.4% of the expected mass over the collection time (Fig. 4) was

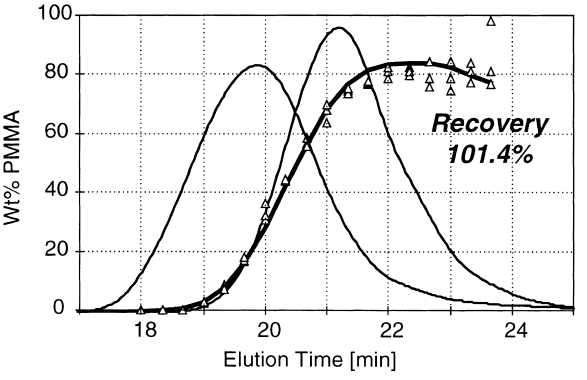

Fig. 8. Calculated 50:50 PS/PMMA blend composition using LR external calibration expressed as weight percent PMMA of annealed SEC fractions obtained from the solvent–evaporation interface. The heavy solid line indicates the weight percent PMMA calculated from DRI data. Data points are from three replicate SEC experiments.

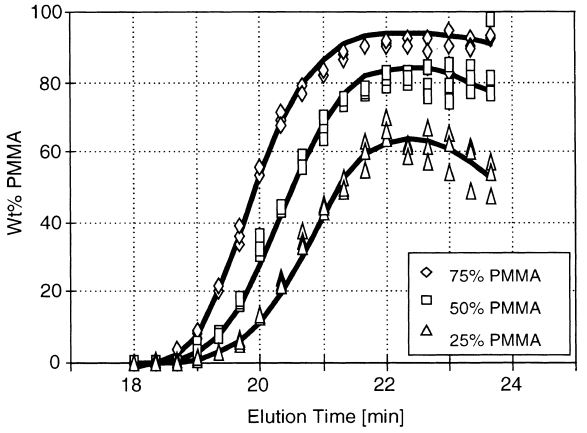

Fig. 9. Comparison of wt% PMMA across the SEC chromatograms determined by FTIR LR external calibration LR:E1 (data points) and DRI (solid lines).

found for the three replicates. This clearly indicates that within experimental precision, the entire SEC eluate sample was deposited on the Ge collection disks. This lends confidence to the potential for use of the internal calibration approach discussed below (LR:I and PLS:I).

Further analysis of the accuracy of the FTIR quantitation was evaluated by comparing the bias between the DRI expected blend composition and that determined by FTIR. Fig. 10 shows the relative percent error (Eq. (1)) of the calculated Wt% PMMA for each fraction across the SEC blend chromatograms. Across the majority of the SEC chromatogram, the relative error in FTIR predicted Wt% PMMA is in the ±10% range with no determinate variation.

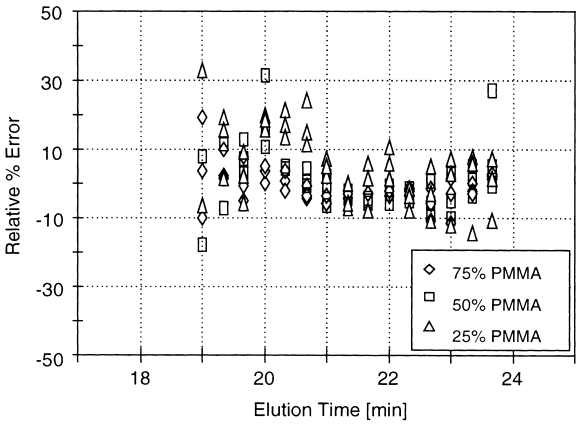

Fig. 10. LR:E1 external calibration relative percent error in wt% PMMA prediction.

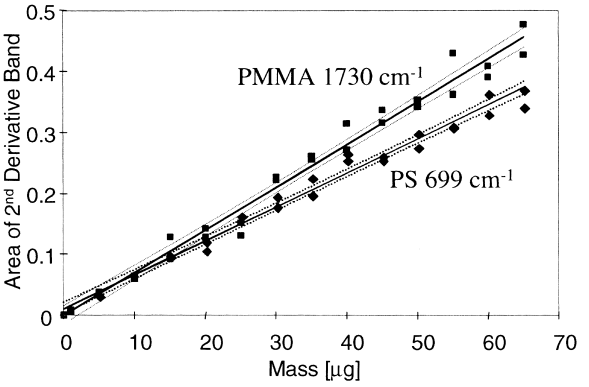

Fig. 11. External calibration plots using peak area of second derivative spectra for PS and PMMA. The dotted lines indicate 95% confidence interval ranges about the regression lines.

LR calibrations with external standards using the area under the doubly differentiated peaks (LR:E2) are shown in Fig. 11. Quantitative prediction of polymer blend compositions was performed in the same manner as LR:E1, with wt% PMMA bias shown in Fig. 12 as relative percent error. A more systematic error in over-prediction of wt% PMMA is observed in the tails of the polymer distribution (Fig. 8). This is attributed to the decreased signal-to-noise provided by second derivative spectra.

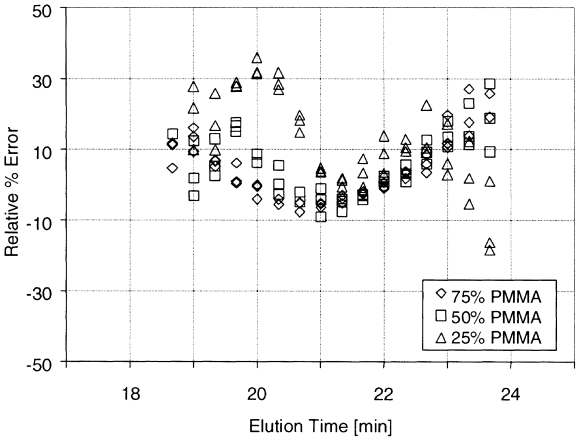

Fig. 12. LR external calibration, peak area of 2nd derivative spectra, LR:E2 relative percent error in wt% PMMA prediction.

5.6. Quantitative analysis of composition across the chromatogram using linear regression and internal calibration (LR:I)

Internal calibration was performed using SEC chromatograms of pure polymer samples. The mass of each polymer fraction obtained with the solvent–evaporation interface on the germanium collection disks was calculated based on the normalized DRI chromatogram of a replicate separation.

Peak areas of second derivative spectra of pure annealed polymers were used to obtain calibration curves. The resulting internal calibration data and LR fits for PS and PMMA are shown in Fig. 13. The relative percent error in blend composition prediction using this approach (LR:I) is shown in Fig. 14. Reasonable accuracy is obtained only near the PMMA maximum concentration (20–22 min). However, a systematic variation in over-prediction of Wt% PMMA is observed at long retention times and very large under-prediction at short retention times. These errors can be directly attributed to the erroneous positive intercepts of the calibration plots of Fig. 13 due to the large scatter in calibration points.

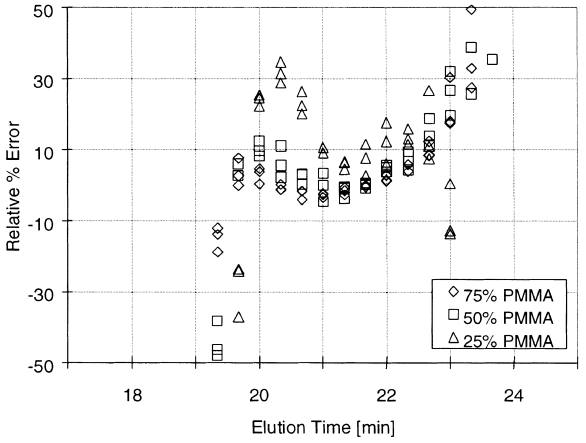

Fig. 14. LR:I internal calibration (second derivative peak area) relative percent error in wt% PMMA prediction.

5.7. Quantitative analysis of composition across the chromatogram using partial least squares and internal calibration (PLS:I)

Without first converting the spectra to second derivative of the absorbance, low absorbance versus mass correlation is observed in the PLS training sets.

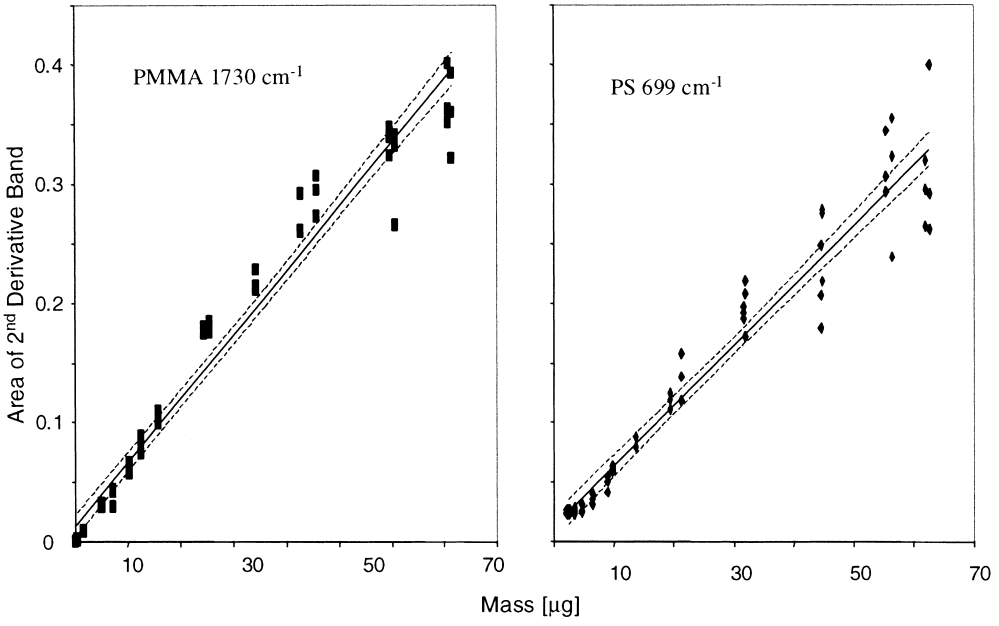

Fig. 13. Internal calibration plots using peak area of second derivative spectra for polymer films obtained from the solvent evaporation interface. The dotted lines indicate 95% confidence interval ranges about the regression lines.

Table 3
PLS training set spectral regions

Spectral range (cm^{-1})	Component	Functional group
3101–3035	PS	aromatic C–H
2981–2962	PMMA	methyl C–H
1755–1705	PMMA	ester carbonyl
1612–1589	PS	phenyl ring
1277–1122	PMMA	ester
713–687	PS	phenyl ring

These low correlations are due to variations in spectral backgrounds related to polymer film thickness variations. Spectral regions for building the PLS training set as shown in Table 3. were selected based on minimum overlap of the component absorbance bands and correlation coefficient values >0.90.

The relative percent errors in blend composition prediction are shown in Fig. 15 for quantitation using a PLS model with internal calibration (PLS:I) using annealed film second derivative spectra. The random error in blend composition prediction here is much lower than is obtained with the LR models. Significant determinate variation is observed in the tails of the polymer distribution. Significant over-prediction of wt% PMMA is observed at both ends of the PMMA distribution. The over-prediction at short retention times is too large to fit on the scale of Fig. 15 and is not shown. As mentioned, it is speculated that this determinate error is due to the degraded signal-to-noise ratio in the second derivative spectra relative to the raw absorbance response used with LR:E1 above.

For comparative purposes, a PLS calibration model was also constructed using the ''as collected'' film spectra prior to solvent annealing and applied to the corresponding blend fraction spectra. These spectra show significant distortions in band shape and relative band intensities due to film non-uniformities (e.g., Fig. 5). The results of the polymer component quantitation are again expressed as relative percent error in predicted wt% PMMA in Fig. 16. Considering the significant spectral distortions, surprisingly small bias is found for all but the lowest percent PMMA blend samples. Increasing determinate variation is observed with decreasing amount of PMMA in the overall blend. These results may overestimate the quality of the PLS quantitation results however, as discussed in the next section.

5.8. Integrated mass accuracy

The previous data was presented in terms of the calculated weight percent of one blend component, PMMA. An additional evaluation of the FTIR quantitation accuracy is provided by observing the bias in the integrated mass across the SEC chromatogram relative to the expected DRI values. Significant variance between quantitation methods is seen in the data plotted in Fig. 17. Table 4 summarizes both bias

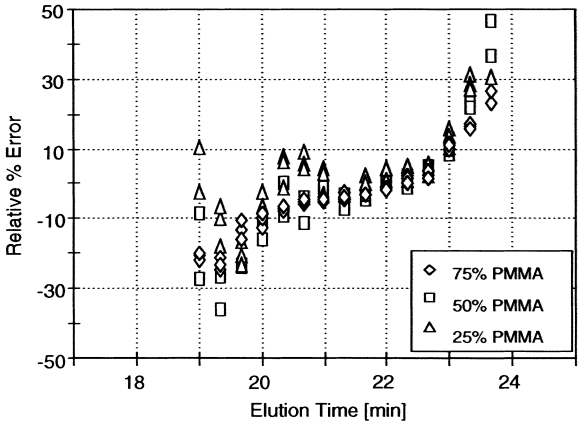

Fig. 15. PLS internal calibration relative percent error in wt% PMMA prediction from annealed film spectra.

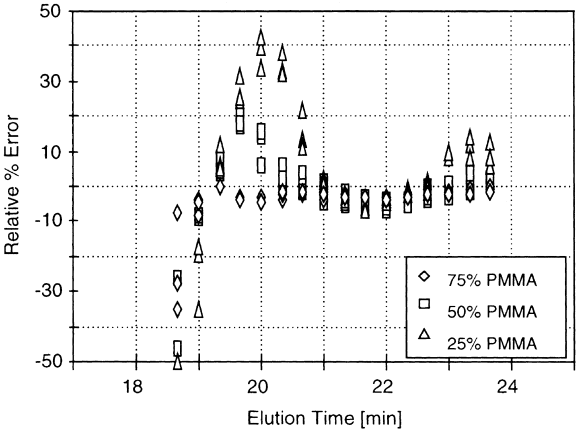

Fig. 16. PLS internal calibration relative percent error in wt% PMMA prediction from ''as collected'' film spectra.

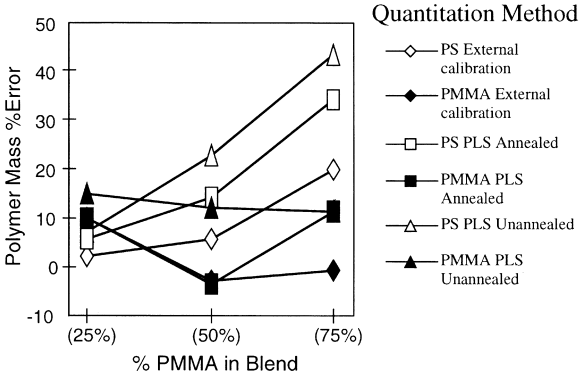

Fig. 17. Comparison of integrated polymer mass results (Eq. (2)) from different quantitation methods.

and precision of the integrated mass results for the blend components.

This provides a direct comparison between the predictions obtained from the three LR calibration models. Note that using external standards, application of second derivative preprocessing (LR:E2 vs. LR:E1) significantly improves accuracy while maintaining predicted mass precision. However, changing from external to internal standardization (LR:I vs. LR:E2) degrades predicted mass precision while maintaining accuracy on average.

6. Conclusions

- Film thickness uniformity is the prime determinant of spectral quality.
- The use of linear regression with external standard calibration provided the best mass accuracy (smallest bias) but relative error in composition was sometimes high because of difficulties in accurately determining band areas. Calculations were labor intensive.
- Application of second derivative preprocessing to LR models did not significantly improve quantitation results or processing time.
- Partial least squares with internal calibration and using annealed samples provided more bias in some quantities than other methods. However, PLS was about equilavent in precision and much less time consuming to implement than the others. Furthermore, as will be seen in subsequent publications [16,17] more discriminating selection of wavelength range greatly reduces bias. When samples were not annealed relative error was low. However, this effect is expected to be sample dependent because it actually uses scattering by the film to assist the composition determination. While experimental work was minimized, mass accuracy was worst for quantitation using spectra without prior solvent annealing of collected polymer films.

References

[1] C.W. Saunders, L.T. Taylor, Appl. Spectrosc. 45 (1991) 900.
[2] K. Nishikida, T. Housaki, M. Morimoto, T. Kinoshita, J. Chromatogr. 517 (1990) 209.
[3] S. Bourne, Am. Lab. 30 (1998) 17F.
[4] J.N. Willis, J.L. Dwyer, M.X. Liu, Int. J. Polym. Anal. Charact. 4 (1997) 21.
[5] P. Tackx, S. Bremmers, Polym. Mater. Sci. Eng. 78 (1998) 50.
[6] T.C. Schunk, T.E. Long, J. Chromatogr. A 692 (1995) 221.
[7] P. Cheung, S.T. Balke, T.C. Schunk, T.H. Mourey, J. Appl. Polym. Sci., Appl. Polym. Symp. 52 (1993) 105.

Table 4
Comparison of bias and precision of integrated polymer mass for both blend components using different quantitation methods

Calibration approach	PS bias (%)	PS mass precision CV_m [a] (%)	PMMA bias (%)	PMMA mass precision CV_m [a] (%)
LR:E1	9.28	2.64	2.12	4.17
LR:E2	2.49	3.94	−0.32	4.59
LR:I	7.74	6.89	4.24	5.54
PLS:I annealed	18.1	2.92	3.35	3.65
PLS:I ''as collected''	24.4	3.24	13.0	3.32

[a] CV_m calculated as the RMS of the values obtained for the three blend compositions.

[8] T.C. Schunk, S.T. Balke, P. Cheung, J. Chromatogr. A 661 (1994) 227.
[9] P.C. Cheung, S.T. Balke, T.C. Schunk, in: T. Provder, H.G. Barth, M.W. Urban (Eds.), Chromatographic Characterization of Polymers Hyphenated and Multidimensional Techniques, ACS, Washington, DC, 1995, pp. 265–279, Adv. Chem. Series 247.
[10] P.C. Cheung, S. Hsu, M. Tempel, S.T. Balke, T.C. Schunk, L. Li, S. Sosnowski, M.A. Winnik, Int. J. Polym. Anal. Char. 2 (1996) 271.
[11] A.L. Smith, in: Applied Infrared Spectroscopy: Fundamentals, Techniques, and Analytical Problem-Solving, John Wiley and Sons, New York, 1979, p. 78.
[12] D.N. Kendall, in: D.N. Kendall (Ed.), Applied Infrared Spectroscopy, Reinhold, New York, 1966, pp. 137–138.
[13] H.W. Siesler, K. Holland-Moritz, Infrared and Raman Spectroscopy of Polymers, Marcel Dekker, New York, 1980.
[14] H. Martens, T. Naes, Multivariate Calibration, J. Wiley, New York, 1989.
[15] A.H. Dekmezian, T. Moroika, C.E. Camp, J. Polym. Sci. Part B Polym. Phys. 28 (1990) 1903.
[16] K. Torabi, S.T. Balke, T.C. Schunk, Proceedings of Intern. GPC Symp., Waters Corp., 1999, pp. 167–188.
[17] A. Karami, S.T. Balke, T.C. Schunk, J. Chromatogr., in press.